

Experimental demonstration of both inverted and non-inverted wavelength conversion based on transient cross phase modulation of SOA

Songnian Fu, Jianji Dong*, P. Shum, and Liren Zhang

(1) Network Technology Research Centre, Nanyang Technological University, 637553, Singapore

*Also with the affiliation (2)

Xinliang Zhang, and Dexiu Huang

(2) Wuhan National Laboratory for Optoelectronics, Huazhong University of Science and Technology, Wuhan, 430074, China

jjdong@mail.hust.edu.cn

Abstract: We demonstrate experimentally ultrafast inverted and non-inverted wavelength conversion (WC) based on a semiconductor optical amplifier (SOA) and an optical bandpass filter (OBF). In the case of small detuning, the WC is inverted regardless if the OBF is blue- or red-shifted with respect to the central wavelength of the converted signal. However the WC is non-inverted when the filter detuning is relatively large. An analytical formula for the transient cross phase modulation is applied to reveal the polarity variation of WC with respect to the OBF detuning. The theoretical detuning values are in good agreement with our experimental results.

©2006 Optical Society of American

OCIS codes: (060.4510) Optic communication; (250.5980) Semiconductor optical amplifier.

References and links

1. T. Houbavlis, K. E. Zoiros, M. Kalyvas, G. Theophilopoulos, and C. Bintjas, "All-optical signal processing and applications within the esprit project DO_ALL," *J. Lightwave Technol.* **23**, 781-801 (2005).
2. S. Nakamura and K. Tajima, "Ultrafast all-optical gate switch based on frequency shift accompanied by semiconductor band-filling effect," *Appl. Phys. Lett.* **70**, 3498-3500 (1997).
3. S. Nakamura, Y. Ueno, and K. Tajima, "Ultrafast all-optical switching based on frequency shift accompanied by the semiconductor band-filling effect," *IEEE LEOS '98*. 160-161 (1998).
4. J. Leuthold, D. M. Marom, S. Cabot, J. J. Jaques, and R. Ryf, "All-optical wavelength conversion using a pulse reformatting optical filter," *J. Lightwave Technol.* **22**, 186-192 (2004).
5. Y. Liu, E. Tangdionga, Z. Li, S. Zhang, and H. deWaardt, "Error-free all-optical wavelength conversion at 160 Gb/s using a semiconductor optical amplifier and an optical bandpass filter," *J. Lightwave Technol.* **24**, 230-236 (2006).
6. Y. Liu, E. Tangdionga, Z. Li, H. deWaardt, and A. M. J. Koonen, "Error-free 320 Gb/s SOA-based wavelength conversion using optical filtering," *OFC 2006 PDP28* (2006).
7. M. L. Nielsen, B. Lavigne, and B. Dagens, "Polarity-preserving SOA-based wavelength conversion at 40 Gbit/s using bandpass filtering," *Electron. Lett.* **39**, 1334 - 1335 (2003).
8. J. Dong, S. Fu, P. Shum, X. Zhang, H. Liu, and D. Huang, "Modeling of SOA-based high speed all-optical wavelength conversion with optical filter assistance," *IEEE NUSOD 2006 WA4* (2006)
9. J. Dong, X. Zhang, Z. Jiang, and D. Huang, "Theoretical and experimental study on all-optical wavelength converters based on the single-port-coupled SOA," *Optical and Quantum Electron.* **37**, 1011-1023 (2005).

1. Introduction

All-optical wavelength conversion (WC) based on semiconductor optical amplifiers (SOAs) has received considerable attention during the past years in terms of small footprint, low power consumption, and optical integration [1]. However, the relatively slow gain recovery time of SOAs limits the maximum operation speed. Currently all-optical WC based on

transient cross phase modulation (T-XPM) of SOAs is a promising technique for high speed WC [2-3]. When a data stream with ultrashort pulsewidth is mixed with a continuous wave (CW) probe signal and injected into SOA, the optical spectrum of the probe signal will be broadened due to transient nonlinear phase shift. A consequent optical bandpass filter (OBF) can then be applied to select the different frequency components of the probe signal. The mechanism of the T-XPM not only provides ultrafast and high-efficient WC, but also has the advantage of simple configuration [3]. J. Leuthold *et al* first presented a novel WC based on a single SOA followed by an OBF. Both the blue- and red-chirped components of the converted signals are filtered by a pulse reformatting optical filter to achieve WC format conversion [4]. An inverted WC at 160 Gb/s [5] and 320 Gb/s [6] was demonstrated by employing an OBF to select the blue-shifted part of the spectrum of the probe light. At the same time, the 40Gb/s non-inverted WC with the same principle has also been shown [7].

In this paper, we demonstrate that both inverted and non-inverted WCs can be realized when the central wavelength of the OBF is either blue-shifted or red-shifted with respect to the wavelength of the probe light. To the best of our knowledge, it is the first report that both inverted and non-inverted WCs can be realized with a red-shifted OBF. Although Ref. [4] also employed a red-shifted filter, the scheme is implemented by delaying the red-chirped part with respect to the blue-chirped part before recombining them. The effect of splitting off and recombining the two spectral components is the key principle. However the detuned OBF in our configuration is used to extract the fast chirp dynamics component, which leads to ultrafast WC.

2. Experimental results

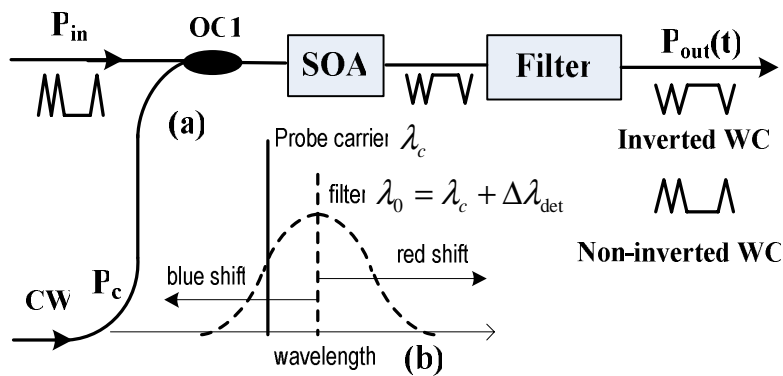


Fig. 1. Schematic diagram for inverted and non-inverted wavelength conversion based on SOA and optical bandpass filter. (a) Setup for wavelength conversion. (b) The optical spectrum of the input probe signal and the filter shape.

The operation principle for WC based on T-XPM of SOA is described in Fig. 1(a). An ultrafast pulse-stream with power P_{in} is combined with a CW probe light P_c , and launched into the SOA. The input data signal will induce transient nonlinear phase shifts to the probe signal via cross phase modulation in the SOA. As a result, the optical spectrum of the probe signal will be broadened. The purpose of the subsequent OBF is to take the signal component at the central wavelength $\lambda_c + \Delta\lambda_{det}$, where $\Delta\lambda_{det}$ is the detuning value from probe wavelength λ_c . Note that the positive/negative value of $\Delta\lambda_{det}$ should be considered as the OBF red-shifted/blue-shifted. Whether the output converted signal is inverted or non-inverted depends on the detuning value $\Delta\lambda_{det}$.

The experimental setup to verify the principle of T-XPM is schematically shown in Fig. 2. The optical data signal is generated by an actively mode-locked fiber laser (AMLFL) at 1550nm wavelength with a 10GHz repetition rate. The optical pulses are externally modulated

with a pseudorandom bit sequence (PRBS) with length 2^7-1 using a Mach-Zender modulator (MZM) and are amplified to 6dBm average power by EDFA 1 before being injected into the SOA. The pulses generated from the AMLFL are approximately 10ps wide. Subsequently the optical pulse-streams are combined with a CW probe signal and launched into the SOA. The probe signal is provided by a tunable laser source, where both wavelength and optical power are fixed at 1556.5nm and 0dBm for the ease of analysis. The isolator in our configuration ensures unidirectional propagation of the combined signals. The SOA (INPHENIX IPSAD1503) was polarization insensitive (~ 0.5 dB typically), therefore no polarization controller (PC) is employed in our configuration. When two mixed signals are injected into the SOA biased at 200mA, the probe signal spectrum will be broadened. Figure 3(a) shows the

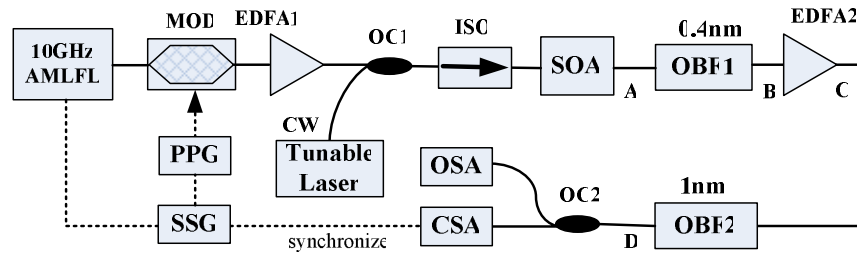


Fig. 2. Experimental setup of wavelength conversion based on a SOA followed by an OBF. AMLFRL: actively mode-locked fiber laser; MOD: modulator; EDFA: erbium-doped fiber amplifier; OC: optical coupler; ISO: isolator; SOA: semiconductor optical amplifier; OBF: optical bandpass filter; OSA: optical spectrum analyzer; CSA: communication signal analyzer; PPG: pulse pattern generator; SSG: synthesized signal generator.

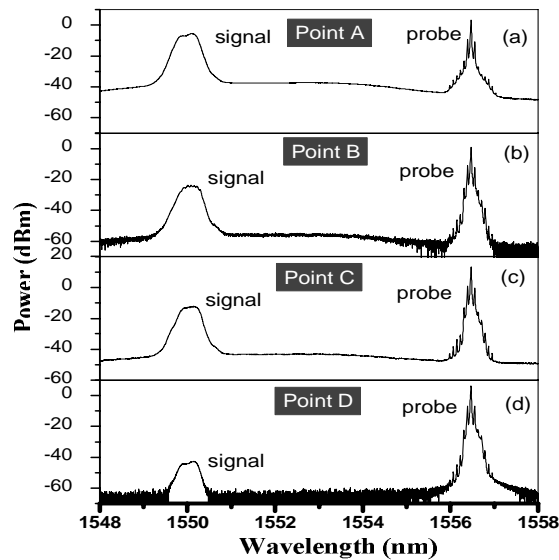


Fig. 3. The optical spectrum measurement at the different position of Fig. 2

spectrum of mixed signals at SOA output. The broadened probe spectrum is mainly caused by cross phase modulation and frequency chirp. The 3dB bandwidth of the subsequent OBF1 is 0.4nm, whose central wavelength is fixed at 1556.5nm. After filtered by OBF1, the data signal at 1550nm is suppressed and the power ratio of the probe and data signal is 25dB, as shown in Fig. 3(b). Another low-noise EDFA 2 is applied to amplify the output probe signal to 13dBm average power. It should be noticed that the data signal is also amplified at the same time, as shown in Fig. 3(c). Then, we apply another filter-OBF2 with 1nm bandwidth to suppress the

data signal power. At the output of OBF2, we measure the optical spectrum, as shown by Fig. 3(d). We find the power ratio of the probe and data signal is larger than 56dB, and the peak power of the probe signal is 6dBm. The crosstalk between probe and data signal is avoided due to presence of OBF2. Finally, the optical spectrum analyzer (OSA) and communication signal analyzer (CSA) can be used to observe the optical spectrum and waveform of the converted signal. Note that, in the experiment, we tune the wavelength of the probe to change the relative position of the filter with respect to the probe without adjusting the filter central wavelength.

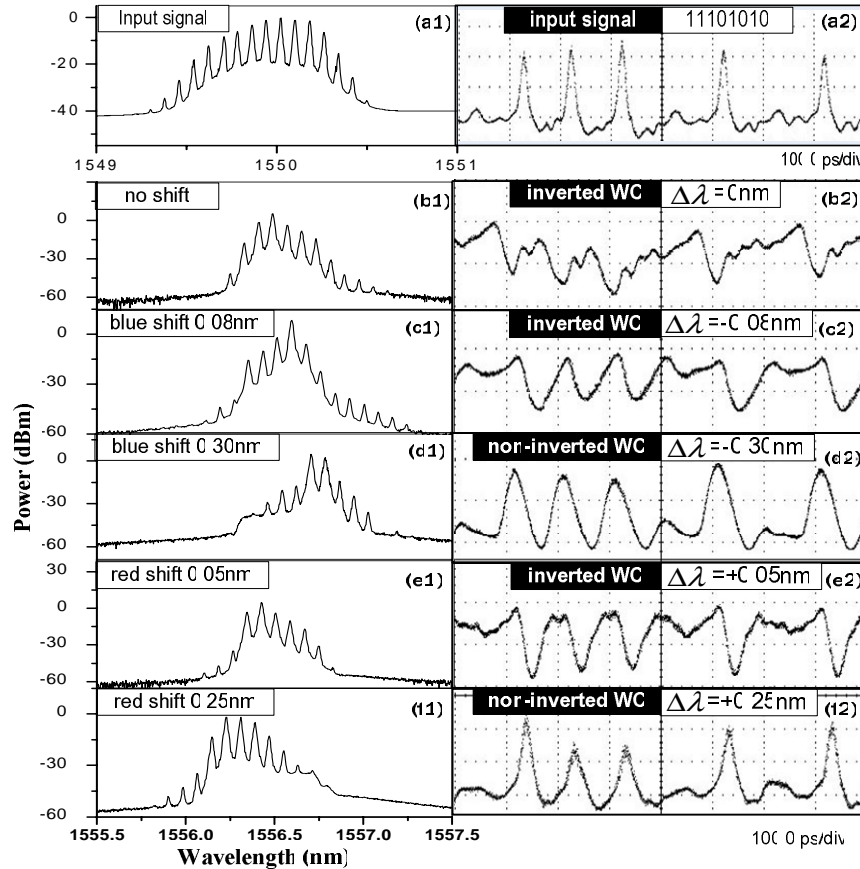


Fig. 4. The wavelength conversion results with respect to the different detuning value of filter when the input data stream is “11101010”. (a) Original waveform of input signal; (b) inverted wavelength conversion on the condition of no filter detuning; (c) inverted wavelength conversion on the condition of filter blue-shifted 0.08nm; (d) non-inverted wavelength conversion on the condition of filter blue-shifted 0.3nm; (e) inverted wavelength conversion on the condition of filter red-shifted 0.05nm; and (f) non-inverted wavelength conversion on the condition of filter red-shifted 0.25nm.

Figures 4(a1). and 4(a2) show the spectrum and waveform of input data signal. The actively mode- locked fiber ring laser is modulated at 10GHz with 10ps pulsewidth return-to-zero (RZ) format, and therefore the wavelength span between two peaks is 0.08nm. The input data stream is sampled as “11101010”. Figures 4(b1) and 4(b2) are the spectrum and waveform of converted signal without OBF detuning. We find the WC is the conventional inverted WC based on cross gain modulation (XGM) and the recovery time is calculated about 80ps. This relatively slow recovery limits the SOA operation speed. Figures 4(c1) and

4(c2) are the spectrum and waveform of converted signal when the detuning $\Delta\lambda_{\text{det}} = -0.08\text{nm}$. The output waveform is inverted WC. Compared with the original 80ps recovery time without detuning, the recovery time is reduced to 60ps, and the level “1” can recover effectively. From the spectrum, the probe carrier at 1556.58nm is not suppressed by the filter, which leads to inverted WC. Figures 4(d1) and 4(d2) are the spectrum and waveform of converted signal when $\Delta\lambda_{\text{det}} = -0.30\text{nm}$. From the spectrum we find the probe carrier is suppressed by the filter, therefore the output is non-inverted WC. Figure 4(e1) and 4(e2) are the spectrum and waveform of converted signal when $\Delta\lambda_{\text{det}} = 0.05\text{nm}$. In Fig. 4(e1), the probe carrier is located in the bandpass of filter, therefore the output waveform is inverted WC and the recovery time is about 44ps, as shown in Fig. 4(e2). Figure 4(f1) and 4(f2) are the spectrum and waveform of converted signal when $\Delta\lambda_{\text{det}} = 0.25\text{nm}$. The output wave turns out a non-inverted WC. All output spectra in Fig. 4 are quite different from that of the input pulses. This suggests that the time-bandwidth product and therefore the quality of the wavelength-converted pulses will be degraded. Therefore the output data streams can't sustain to propagation along a subsequent long-haul link.

3. Discussion

In Ref. [8], we derived the analytical formula of output power based on the SOA T-XPM, which is expressed as

$$P_{\text{out}}(t) = P_{\text{in}} \exp\left[-(4\ln 2)\left(\frac{\nu_f - \nu_0 - \Delta\nu(t)}{B_{3dB}}\right)^2\right] \left[g^2(t) + g'(t)^2 (2\ln 2 \frac{\nu_f - \nu_0 - \Delta\nu(t)}{\pi B_{3dB}^2})^2\right] \quad (1)$$

where P_{in} is input power of probe signal, and $\Delta\nu(t) = -\frac{1}{2\pi} \frac{d\Phi}{dt}$ is the chirp variation of the probe signal. $g(t)$ and $\Phi(t)$ are the temporal SOA amplitude gain and nonlinear phase shift, respectively. $g'(t) = dg(t)/dt$ is the differential function of $g(t)$. ν_f and ν_0 are absolute frequency of the OBF and probe signal. B_{3dB} is 3dB bandwidth of OBF. In order to investigate the polarity evolution of WC theoretically, we have to firstly calculate the gain $g(t)$ and frequency shift $\Delta\nu(t)$ with the SOA subsection model [9]. The pump signal at 1550nm has a 6dBm peak power, a 10ps pulsewidth, and a 10GHz repetition rate, meanwhile the probe signal at 1556nm is under CW operation with 0dBm average power. The 3dB bandwidth of the subsequent filter is 0.4nm. The evolutions of the output signal waveforms are plotted according to Eq. (1), as shown in Fig. 5. In the plot, the detuning value of OBF is varied from 0.48nm (-60GHz) to -0.48nm (60GHz). We can observe that the polarity of WC is inverted when detuning value is small, while non-inverted when detuning value is large. The comparisons between the experimental results and the theoretical detuning values are shown in Table 1. Excellent agreement between the calculations based on Eq. (1) and the experimental results is noticed.

In Fig. 4, we notice that the experimental output waveform of converted signal has some distortion. For our proposed scheme, we found the extinction ratio conservation is not possible. For the worst case of inverted WC in Fig. 4(c2), the extinction ratio is degraded from 18dB to 12dB. We also observed that, for the inverted WC, the power level “1” has amplitude jitter, as observed in Fig. 4 (c2) and 4(e2). For the non-inverted WC, the “ghost” pulses appear between the two wider-spaced pulses in Fig. 4(d2) and 4(f2). This is due to fact that the bit “0” of the input signal is not completely suppressed by our MZM. The distortion could be eliminated by using intensity modulator with better polarization stability. We also found that the output pulses become broader compared to the input signal. The reason lies in the fact

that the OBF in our configuration has a narrow bandwidth at 0.4nm. We have theoretically compared the output pulsewidths when the filter 3dB bandwidth is 0.8nm, 0.4nm, and 0.2nm, respectively. And we found that the output pulsewidth will be broadened from 10ps to 24ps if 0.4nm OBF is applied. The power of output signal will increase and the pulsewidth of output signal will become narrower when the filter 3dB bandwidth gets larger. Due to some hardware constraints, our demonstration is limited to a 10GHz repetition rate. However, we believe the operation speed could be over 100Gb/s with pulsewidth less than 2ps [5-6].

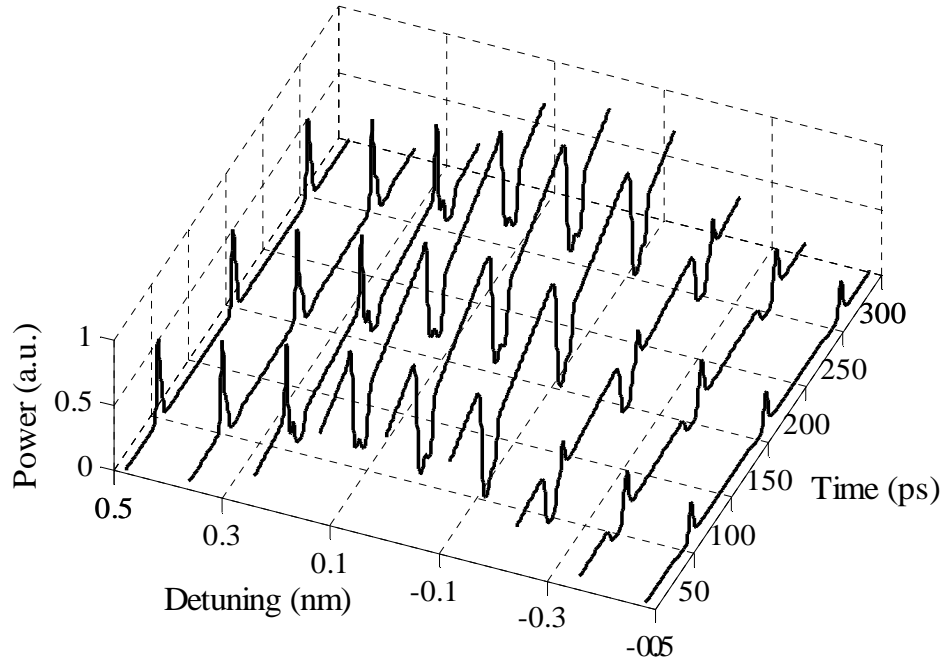


Fig. 4. The waveform evolutions of the output converted signal with respect to the filter detuning value

Table 1. The filter detuning value comparison between experiments and calculations based on Eq. (1).

Polarity	Blue shift/nm		Red shift/nm	
	Experiment	Calculation	Experiment	Calculation
Inverted	0.04-0.08	0.04-0.08	0.05-0.08	0.04-0.12
Non-inverted	0.24-0.3	0.27-0.43	0.25-0.34	0.28-0.52

4. Conclusions

We demonstrate that both inverted and non-inverted WCs can be realized with only one SOA and a 0.4nm OBF. When the detuning of the OBF is small, the WC is inverted and the contribution of XGM is dominant. While the WC becomes non-inverted from the interaction of XGM and T-XPM, when the detuning of OBF is relatively large. An analytical formula for the transient cross phase modulation is applied to reveal the polarity variation of WC with respect to the OBF detuning. The theoretical detuning values are in good agreement with our experimental results.

Acknowledgments

This work is partially supported by the project M47040039 of Agency for Science, Technology and Research (A*STAR), Singapore, and partially supported by National Natural Science Foundation (Grant No. 60407001), P. R. China.